Environmental Earth Sciences _####################_
https://doi.org/10.1007/s12665-019-8394-x

ORIGINAL ARTICLE

Effects of dam construction on total solids in the Ca River, north-central Vietnam

Ho Thi Phuong[1] · Kenji Okubo[2]

Received: 20 April 2018 / Accepted: 1 July 2019

Abstract
The river regime laws of the hydraulic properties of the cross sections of two hydrological stations (Dua and Yen Thuong) along the Ca River in north-central Vietnam were combined into power functions with exponents of 1.46–1.85 using the Manning roughness coefficient and the settling velocity or the particle size to simulate the suspended sediment load. The Nash–Sutcliffe efficiency, percent bias, and the ratio of the root-mean-square error to the standard deviation of the measured data were used to evaluate the calibration process for the pre-dam period (1994–2004) and for validation for the post-dam period (2005–2014). Effects of dam construction include a change in the relationship between the Manning roughness coefficient and sediment particle size. The observed sediment load decreased by approximately 20–40% after dam construction at both stations. We used a power function with exponents of 0.968 and 0.992 for the dissolved solid load to calculate the long-term annual total dissolved solids at the Dua and Yen Thuong stations, respectively. After dam construction, the average value of the total suspended solids–total dissolved solids ratio decreased from 3.0 to 2.3 at the Dua station and from 4.1 to 2.2 at the Yen Thuong station.

Keywords Total solids · Suspended solids · Dissolved solids · Regime laws · Sediment transport · Ca River

Introduction

The total solid load is controlled by Earth system drivers (e.g., climate, basin relief, basin geology, and drainage basin area) (Brinkmann 1989; Meybeck 2003; Milliman and Farnsworth 2011). It has been reported that rivers discharge more than 19 billion tons of solids and 3.8 billion tons of dissolved matters annually into the global ocean (Milliman and Farnsworth 2011). The correlation between particulate and dissolved matters yields demonstrates the dependence of chemical weathering on the extent of physical weathering, which reflects the natural background of particular rivers. This linkage enables approximate hydrogeochemical classification. For example, Brinkmann (1989) classified river water as whitewater, clearwater, blackwater, and mixed waters based on the range and relationship between total dissolved solids and total suspended solids. Milliman and Farnsworth (2011) classified river systems as dissolved-dominated and sediment-dominated according to the total suspended solids–total dissolved solids (TSS–TDS) ratio. These authors reported that dissolved-dominated rivers are particularly prevalent in Europe and Eurasia.

Anthropogenic activities (e.g., river damming) have drastically modified the flux of natural river material (Meybeck 2003). A persistent change in water discharge and sediment load because of dam regulation can result in disequilibrium between supplied sediment and released sediment (Andrews 1986). Consequently, dams can alter natural river regimes (Chien 1985) and modify a river's morphology and riverbed characteristics (Meybeck 2003). A reservoir can regulate river flows by, for example, suppressing floods, raising the base flow, and catching coarse sediments and passing finer silt only (Eiriksdottir et al. 2017; Xu 2007; Yang et al. 2017). When eutrophication occurs in a reservoir, nutrient

Electronic supplementary material The online version of this article (https://doi.org/10.1007/s12665-019-8394-x) contains supplementary material, which is available to authorized users.

✉ Ho Thi Phuong
phuongmt.dhv@gmail.com

[1] School of Chemical, Biological and Environmental Technologies, Vinh University, 182, Le Duan Street, Vinh City, Nghe an, Vietnam

[2] Graduate School Environmental and Life Science, Okayama University, 3-1-1, Tsushima-Naka, Kita-ku, Okayama 700-8530, Japan

Journal : Large 12665 | Article No : 8394 | Pages : 10 | MS Code : 8394 | Dispatch : 4-7-2019

and silicate deficiencies can be observed downstream of the dam. This situation can cause a change in ion constitution and affect biogeochemical cycling in coastal seas (Friedl and Wüest 2002; Humborg et al. 1997).

Located in Southeast Asia, Vietnam possesses one of the largest dam networks in the world. This network comprises more than 7000 dams of different types and sizes (Amos et al. 2017). The Ca River is one of the largest basins in Vietnam, and it currently included numerous dams built for power generation, flood control, and water supply. This study aims to assess the impact of dam construction in the upper Ca River by evaluating the suspended sediment load in a downstream hydrological station. Additionally, this study discusses the suspended sediment transport in the Ca River in north-central Vietnam and compares results with theoretical methods. The research period was divided into a pre-dam period (1994–2004) and a post-dam period (2005–2014) for quantitative comparison. The dissolved solid load is not available for long-term periods, but it is available by applying the loading $L_{DS} - Q$ curves for dissolved solids obtained from field measurements.

Study area and data

The study was performed in the Ca River basin, which is the third largest river in north-central Vietnam, located between 18°15′00″N and 20°10′30″N and 103°45′20″E and 105°15′20″E (Fig. 1). The main flow of the river originates from Mt. Muong Khut and Mt. Muong Lap (1800–2000 m) in Lao People's Democratic Republic (PDR). It runs in a northwest–southeast direction, crossing Lao PDR's Xiangkhouang Province and Vietnam's Nghe An and Ha Tinh provinces, and it flows out into the East Sea through Cua Hoi. The total basin area is 27,200 km^2, including 17,730 km^2 in Vietnam's territory. The main river length is 531 km, of which 170 km runs through Lao PDR and 361 km runs through Vietnam. The river network density is 0.6 km/km^2. The topography of the Ca River AQ2 is very diverse with a general slope in the West–East, Northwest–Southeast, Southwest–Northeast. The mountainous terrain accounts for 60%–70% of the catchment area, which is mainly a watershed protection forest. Midland hills have a height of 20 m–200 m, accounting for about 25%–35% of the area. The Ca River plain is located along both sides of the river, small and narrow, with the elevation gradually changing from 15 to 0 m, accounting for about 10% of the basin area. In terms of geological characteristics, the area of Ca river fault zone distributes geological formations with early and middle Paleozoic age to Quaternary age. Sedimentary formations occupy most of the area. Soil types are formed from the parent rocks which are concentrated mainly in hilly and mountainous areas; Ferralsol in particular (accounting for 83.51%) (IWRP 2012). Except for the alluvial soils in the low valleys, soils in the area are generally acidic, poor in nutrients, and highly susceptible to erosion (Giang et al. 2007).

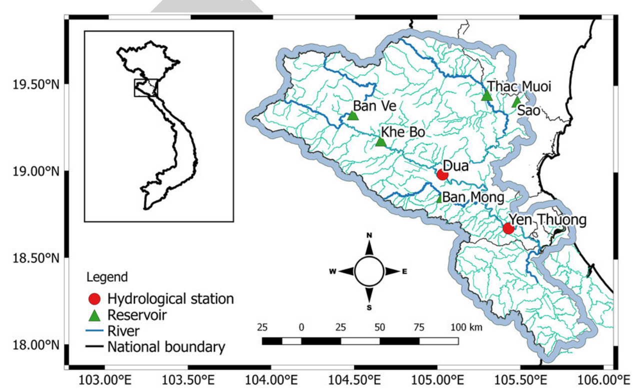

Fig. 1 Map of the Ca River

Many reservoirs have been built in the Ca River basin: the reservoirs of Ban Ve and Khe Bo on the main stream of the Ca River, the Ban Mong reservoir on the Hieu River, and the Sao River reservoir located in a tributary of the Hieu River. These multi-purpose reservoirs are used for hydropower generation, water supply, irrigation, and flood and drought control. The Ban Ve reservoir is the largest hydropower project on the Ca River and also the largest hydropower project in north-central Vietnam. It has a capacity of 320 MW, and construction began at the end of 2005. Additionally, many other reservoirs have been built on small rivers and streams of the Ca River. These reservoirs have a small capacity and are used mainly for irrigation purposes.

In this study, data were collected at the Dua (105°02′20″E and 18°59′20″N) and Yen Thuong hydrological stations (105°23′00″E and 18°41′10″N) during the time period 1994–2014. Both stations are located in the downstream of the Ca River with an elevation of 16 m at Dua station and 4 m at Yen Thuong station. The yearly flow regime is divided into two distinct seasons: flood season (from June to November) and dry season (from December to May). The respective basin areas at Dua and Yen Thuong are 20,800 and 23,000 km^2 (Chikamori et al. 2012). The collected data include daily discharge, hydrological regime, and suspended sediment concentration. The dissolved solids data were not available at both the stations, but electrical conductivity (EC) data at the Dua station were available for several years beginning in 2000. All of the data were provided by the North-Central Hydro-meteorological Centre of Vietnam. The collected data revealed that the mean annual flow ranges between 221 and 902 m^3/s with an average 571 m^3/s at Yen Thuong in 1994–2014. The mean annual flow ranges between 109 and 635 m^3/s with an average 407 m^3/s at Dua.

Journal : Large 12665	Article No : 8394	Pages : 10	MS Code : 8394	Dispatch : 4-7-2019

Methods

Station hydraulic geometry

The relationship between a river's discharge and hydraulic variables such as its width, depth, and velocity in river cross sections are expressed as power functions, which are also described by the term "at-a-station hydraulic geometry" (Leopold and Maddock 1953):

$$b = b_1\hat{Q}^{b_0},\ \ h = h_1\hat{Q}^{h_0},\ \ \bar{u} = u_1\hat{Q}^{u_0},\ \ b_1h_1u_1 = 1,\ \ b_0 + h_0 + u_0 = 1, \tag{1}$$

where b, h, and $\bar{u}$ are the width, depth, and average velocity, respectively, of the river's cross section. The normalized discharge is $\hat{Q} = Q/Q_1 = \bar{u}bh/u_1b_1h_1$ and b_1, h_1, and u_1 represent the dimensional intercepts of the regime curves at $Q = Q_1$, the unit discharge. The values b_0, h_0, and u_0 are the power exponents of discharge related to the width, depth, and average velocity, and they also represent the slope of the regime laws.

Calculation of suspended sediment load

In this study, suspended sediment load was estimated using a hydrological approach. We adopted the hydraulic geometry of Leopold and Maddock (1953) by making a dimensional consideration and using the concentration formula given by Celik and Rodi (1991) and an average velocity of the river's cross section. As a result, the suspended sediment load formula only depends on Manning's roughness coefficient and particle size. The calculation of suspended sediment load is as follows:

Suspended sediment discharge is estimated by Eq. (2):

$$L_{ss} = \bar{c}\rho_s\bar{u}bh, \tag{2}$$

where L_{ss} [kg/s] is the sediment discharge, Q [m^3/s] is water discharge, $\rho_s = 2650$ [kg/m^3] is the sediment density, $\bar{c}$ is the average volumetric concentration of suspended sediment, $\bar{u}$ [m/s] is the flow velocity, h [m] is the depth, and b [m] is the width of the channel.

The bulk sediment concentration can be replaced by that of the maximum possible transport $\bar{c}$, with which no sedimentation occurs along the river, as given by Celik and Rodi (1991):

$$\bar{c} = 0.034\frac{u_*^2\bar{u}}{\sigma g h w_s}, \tag{3}$$

where u_* is the friction velocity [m/s] that is assumed to be a constant,$\sigma = 1.65$ is the submerged specific weight, w_s is the settling velocity [m/s], and $g = 9.8$ [m/s^2] is the gravitational acceleration.

The friction velocity and the Manning equation are given by:

$$u_* = \sqrt{gRI_e}, \tag{4}$$

$$\bar{u} = n^{-1}R^{2/3}I_e^{1/2}, \tag{5}$$

where R is the hydraulic radius, I_e is the energy grade, and n is Manning's roughness coefficient. Replacing R by h and adapting Eqs. (3)–(5) to Eq. (2), the suspended sediment discharge can be re-written as follows:

$$L_{ss} = 0.034\frac{\rho_s n^2}{\sigma w_s}\bar{u}^4bh^{-1/3} = \frac{54.6n^2}{w_s}\bar{u}^4bh^{-1/3} \tag{6}$$

The regime law, Eq. (1), is used in the equations above to obtain the suspended sediment discharge as follows:

$$L_{ss} = \frac{54.6n^2}{w_s}\bar{u}_1^4b_1h_1^{-1/3}Q^{4u_0+b_0-h_0/3} \tag{7}$$

We used Eq. (7) to estimate suspended sediment load. As shown in the equation, sediment load depends on Manning's roughness coefficient, settling velocity, and major hydraulic characteristics.

The settling velocity is estimated based on the suspended non-cohesive particle size (Habini 1994):

$$w_s = \begin{cases} \sigma g D^2/18\nu & \text{for } D \le 0.1\text{ mm} \\ (10\nu/D)\left\{\left[1 + (0.01\sigma g D^3/\nu^2)\right]^{0.5} - 1\right\}, & \\ \quad \text{for } 0.1\text{ mm} < D < 1.0\text{ mm} & \\ 1.1(\sigma g D)^{0.5} & \text{for } 1.0\text{ mm} \le D \end{cases} \tag{8}$$

where D is sediment particle size [m] and $\nu = 10^{-6}$ [m^2/s] is kinematic viscosity of water.

Efficiency criteria used for calibration and validation of simulated suspended sediment load

Calibration and validation of the suspended sediment load using the simulated equation (Eq. 7) were performed using observed data of the sediment load and hydraulic characteristics recorded at the gauging stations over the course of 20 years (1994–2014). Eleven years of the pre-dam construction period (1994–2004) were used for calibration, and 10 years of the post-dam construction period (2005–2014) were used for validation. The model was calibrated by changing Manning's roughness coefficient between 0.01 and 0.02. The values of the roughness coefficient were selected based on the guideline of Schall et al. (2008). In which, the study sites are classified as "an alluvial sand bed, with no vegetation or plane bed with a Froude number less than

Journal : Large 12665 | Article No : 8394 | Pages : 10 | MS Code : 8394 | Dispatch : 4-7-2019

unity". The calibration process selects the sediment particle size where the efficiency criteria reveal the most appropriate results.

Based on the recommendation of Moriasi et al. (2007), three efficiency criteria—the Nash–Sutcliffe efficiency (NSE), the percent bias (PBIAS), and the ratio of the root-mean-square error to the standard deviation of the measured data (RSR)—were used to evaluate the suspended sediment predictions. The sediment prediction can be judged as "satisfactory" for a monthly time step if $\mathrm{NSE} > 0.50$, $\mathrm{RSR} \le 0.70$, and $\mathrm{PBIAS} \le \pm 55\%$; "good" if $0.65 < \mathrm{NSE} \le 0.75$, $0.50 < \mathrm{RSR} \le 0.60$, and $\pm 15\% \le \mathrm{PBIAS} \le \pm 30\%$; "very good" if $0.75 < \mathrm{NSE} \le 1.00$, $\mathrm{PBIAS} < \pm 15\%$, and $0.00 \le \mathrm{RSR} \le 0.50$; and "unsatisfactory" if $\mathrm{NSE} \le 0.50$, $\mathrm{RSR} > 0.70$ and $\mathrm{PBIAS} \ge \pm 55\%$ (Giang et al. 2017; Moriasi et al. 2007).

$$\mathrm{NSE} = 1 - \frac{\sum_1^n \left(SS_{\mathrm{obs}} - SS_{\mathrm{cal}}\right)^2}{\sum_1^n \left(SS_{\mathrm{obs}} - \overline{SS}_{\mathrm{obs}}\right)^2}, \tag{9}$$

$$\mathrm{RSR} = \frac{\mathrm{RMSE}}{\mathrm{STDEV}^{\mathrm{obs}}} = \frac{\sqrt{\sum_1^n (\mathrm{SS}_{\mathrm{obs}} - \mathrm{SS}_{\mathrm{cal}})^2}}{\sqrt{\sum_1^n (\mathrm{SS}_{\mathrm{obs}} - \overline{\mathrm{SS}}_{\mathrm{obs}})^2}}, \tag{10}$$

$$\mathrm{PBIAS} = \frac{\sum_1^n (\mathrm{SS}_{\mathrm{obs}} - \mathrm{SS}_{\mathrm{cal}})}{\sum_1^n \mathrm{SS}_{\mathrm{obs}}} \times 100, \tag{11}$$

where $\mathrm{SS}_{\mathrm{obs}}$ is the observed daily sediment load, $\mathrm{SS}_{\mathrm{cal}}$ is the calculated daily sediment load, $\overline{\mathrm{SS}}_{\mathrm{obs}}$ is the mean observed daily sediment load, and n is the total number of observations.

Electrical conductivity and total dissolved solids

Electrical conductivity is a measure of the capacity of water to conduct electrical current. Because conductivity is affected by temperature, it is reported at 25 °C (i.e., the specific conductance). Because it is a volume measure of ionized solids, EC can be used to estimate TDS. The relationship between TDS and the specific conductance of water can be approximated by the following equation:

$$\mathrm{TDS} = k_{\mathrm{e}} \times \mathrm{EC}, \tag{12}$$

where TDS is expressed in mg/L and the EC is in microSiemens per centimeter at 25 °C. The correlation factor k_{e} varies between 0.5 and 0.9 (typically 0.7) (Walton 1989). In this study, we used a correlation factor k_{e} of 0.65 (Thirumalini and Joseph 2009). The quantity of the dissolved solids transported by the river, expressed in kg/s, was determined by multiplying the concentration of the dissolved solids by the instantaneous discharge. The loading L_{DS}–Q curve for the dissolved solids was obtained from the analyzed data.

A long-term record of TDS was not available for the Ca River basin. Therefore, historical EC data were used to investigate changes in TDS after dam construction. At the research site, EC data for the Dua station were available once a month from 2000 to 2013. Additionally, to calculate the present TDS load, EC loggers (Model U24-001, HOBO®, Onset Computer Corporation, United States) and model U20-001-01 water level data loggers (HOBO®) were installed at the Dua station from July 1, 2016 through August 31, 2016 and at the Yen Thuong station from June 23, 2016 through March 29, 2017. Electrical conductivity measurements were taken at 1-h intervals. Water level data were used to calculate the discharge using the regime law.

Results and discussion

Hydraulic geometry characteristics at the cross-sectional scale

The relationship between hydraulic variables and discharge at the hydrological stations in the Ca River basin for the entire period of 1994–2014 is shown in Fig. 2. The exponents and coefficients of the hydraulic geometry parameters at each station are listed in Table 1. At Dua station, the width of the river was constant (approximately 250 m throughout the discharge range); the depth and velocity increased progressively as power-law functions of the discharge. The depth increased with the discharge faster than the velocity ($h_{\mathrm{o}} > u_{\mathrm{o}}$). The scatter around the plots occurs both in the lower-flow regime and in the upper-flow regime; this scatter derives from measurement errors, analytical errors, random variations, and systematic changes to the channel (Knighton 1977, 1987). At Yen Thuong station, the velocity increased with the discharge faster than the depth, and the depth increased faster than the width ($u_{\mathrm{o}} > h_{\mathrm{o}} > b_{\mathrm{o}}$) when the discharge was less than 2000 m^3/s. However, the depth increased with the discharge faster than the velocity ($h_{\mathrm{o}} > u_{\mathrm{o}}$); only the width remained constant around 410 m when the discharge exceeded 2000 m^3/s. A marked transition in river width and depth occurs at the Yen Thuong station, but the velocity of the river water is not affected for discharges exceeding approximately 2000 m^3/s. Lewis (1966) and Knighton (1987) noted the type of discontinuity in hydraulic geometry (similar to Yen Thuong) related to lower-flow channelization. At higher flows, the rapid increase in water-surface width leads to a discontinuation of the flow regime, which is commonly associated with overtopping the channel banks and occupation of the adjoining floodplain. Therefore, a new relationship with the discharge

Journal : Large 12665	Article No : 8394	Pages : 10	MS Code : 8394	Dispatch : 4-7-2019

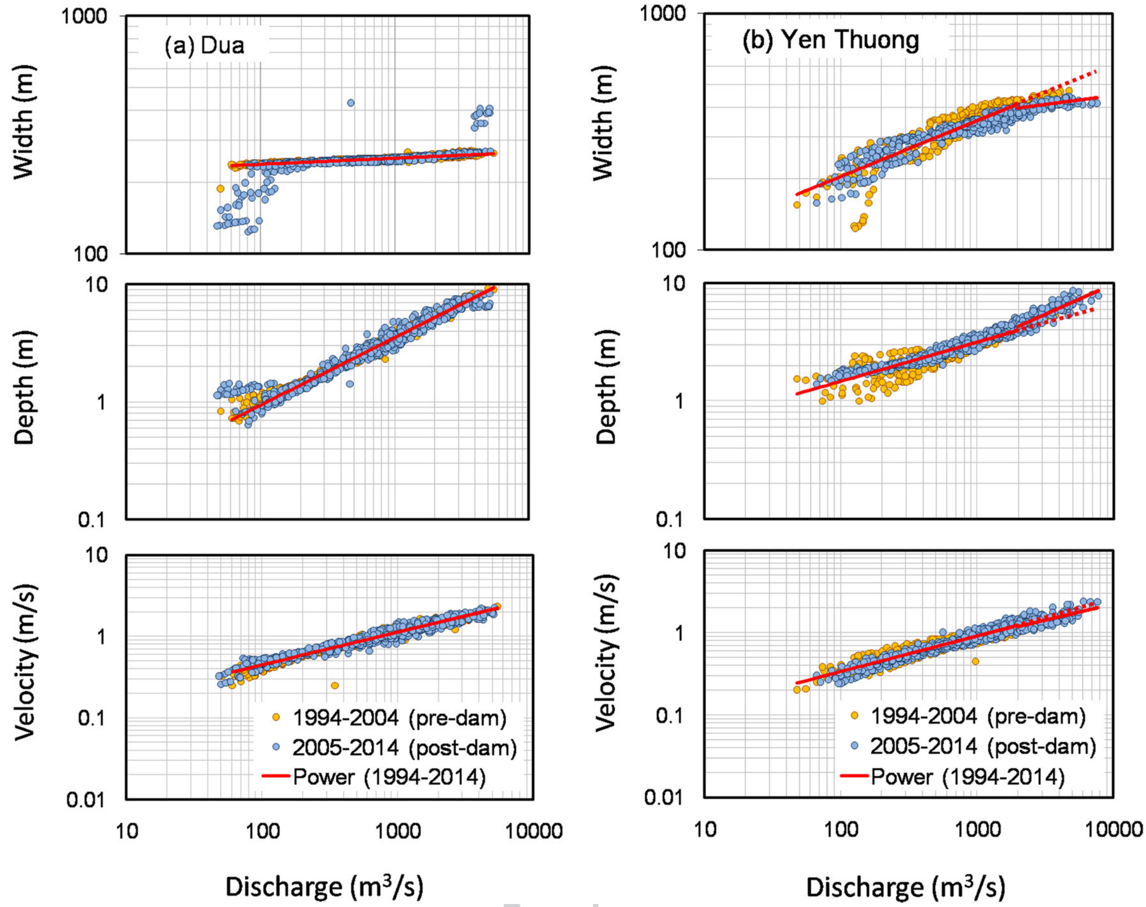

Fig. 2 Relationship of width, depth, and velocity to discharge at Dua (**a**) and Yen Thuong (**b**)

Table 1 The exponents and coefficients of at-a-station hydraulic geometry parameters

Stations	Exponents			Coefficients			$u_o+h_o+b_o$	$u_1h_1b_1$
	u_o	h_o	b_o	u_1	h_1	b_1		
Dua	0.400	0.574	0.026	0.071	0.067	211.00	1.000	1.004
Yen Thuong ($Q<2000$ m^3/s)	0.431	0.332	0.236	0.046	0.316	68.54	0.999	0.996
Yen Thuong ($Q>2000$ m^3/s)	0.396	0.523	0.079	0.058	0.080	217.04	0.998	1.007

develops (Knighton 1987; Leopold and Maddock 1953). The discontinuity in hydraulic geometries can cause more than one break in the slope of the loading curve when the bank profile is highly irregular (Knighton 1987; Richards 1976). Ferguson (1986) concluded that “at-a-station hydraulic geometry” is a function of the shape of the channel.

Changes in the relationship among the hydraulic variables with discharge are compared between the pre-dam period (1994–2004) and the post-dam period (2005–2014) in Fig. 2. The results reveal no significant changes in channel characteristics associated with dams at Dua station. However, an effect of dam construction on channel depth and width was observed at Yen Thuong station. The depth increased at discharges exceeding 2000 m^3/s during the post-dam period; the width of the river narrowed at the upper regime after dam construction. The depth during the post-dam period increased slightly, and there were fewer variations in lower discharges than during the pre-dam period.

Calibration and validation of the suspended sediment load

The parameters of hydraulic geometry listed in Table 1 can be used in Eq. 7. The suspended sediment load is calculated as $L_{ss}=0.54\,n^2w_s^{-1}Q^{1.46}$ for the Dua catchment and $L_{ss}=0.02\,n^2w_s^{-1}Q^{1.85}$ if $Q<2000$ m^3/s and $L_{ss}=0.31\,n^2w_s^{-1}Q^{1.49}$ if $Q>2000$ m^3/s for the Yen Thuong catchment.

To calibrate the suspended sediment load, the Manning roughness coefficient (n) is assumed to be a constant (0.015). The calibration process yielded the best values of the evaluation indices NSE, RSR, and PBIAS, which correspond to the optimal values of sediment diameters. The calibrated parameters were used to validate the post-dam period. Table 2 lists the calibrated and validated parameters. At Dua station, the best values of the NSE, RSR, and PBIAS indices were 0.708, 0.541, and 9% for a sediment particle size of 86 µm; the corresponding values were 0.591, 0.640, and 18% at Yen Thuong for a sediment particle size of 81 µm. The calibration process for sediment predictions can be judged as "satisfactory" to "very good" based on the procedure of Moriasi et al. (2007). The validated values of NSE, RSR, and PBIAS were 0.240, 0.872, and −26% at Dua and 0.090, 0.954, and −41% at Yen Thuong. Most of the evaluation index results were unsatisfactory for the post-dam period at both stations. A comparison of the observed and calculated sediment load (line 1:1 in Fig. 3) indicates that the observed sediment decreased after dam construction.

Table 2 Calibration and validation results of the suspended sediment load at $n=0.015$

Indices	Dua		Yen Thuong	
	Calibration 1994–2004	Validation 2005–2014	Calibration 1994–2004	Validation 2005–2014
*n**	*249*	*225*	*158*	*166*
D (µm)	86	86	81	81
NSE	0.708	0.240	0.591	0.090
RSR	0.541	0.872	0.640	0.954
PBIAS (%)	9	−26	18	−41

*Number of suspended solids samples

Sediment discharge was numerically integrated using the log + linear profile in velocity and the equilibrium concentration profile described by Itakura and Kishi (1980). The coefficients and exponents were expressed using Manning's roughness coefficient, particle size, and the bed slope using the regression technique of Kazama et al. (2005). This technique was adapted for Dua and Yen Thuong along the Ca River. The results were obtained using the calibrated parameters $n=0.015$ and $D=0.0008$ m; the bed slope was assumed to be $I=1/20{,}000$. Kazama et al. (2005) used the load–discharge (L–Q) relationship assuming that the coefficient K and exponent P were functions of the slope, roughness, and particle size (I, n, and D).

$$Q_{ss} = KQ^{P+1} = KQ^{P}Q \tag{13}$$

Camenen and Larson (2008) derived the following equation using their reference concentration c_R based on laboratory results. This equation may be re-written using the diffusivity as $\mathrm{Ko}=\eta\kappa u_* h$ and the Rouse number, $Z=w_s/\beta\kappa u_*$, where $\eta=1/6$ and $\beta=1$.

$$q_{ss} = U_c c_R \frac{K_0}{w_s}\left\{1-\exp\left[-\frac{w_s}{K_0}h\right]\right\} \tag{14}$$

$$Q_{ss} = bq_{ss} = b\bar{u}c_R h\frac{\eta\kappa u_*}{w_s}\left\{1-\exp\left[-\frac{w_s}{\eta\kappa u_*}\right]\right\} = \frac{C_R\{1-\exp[-Z]\}}{Z}Q \tag{15}$$

A steeper increase in the sediment loads was noted in two references (Fig. 4). In the above calculations, particle size was fixed, which is why Camenen and Larson (2008) reported a strong decay in the lowest regime. Kazama et al. (2005) and Camenen and Larson (2008) showed a different

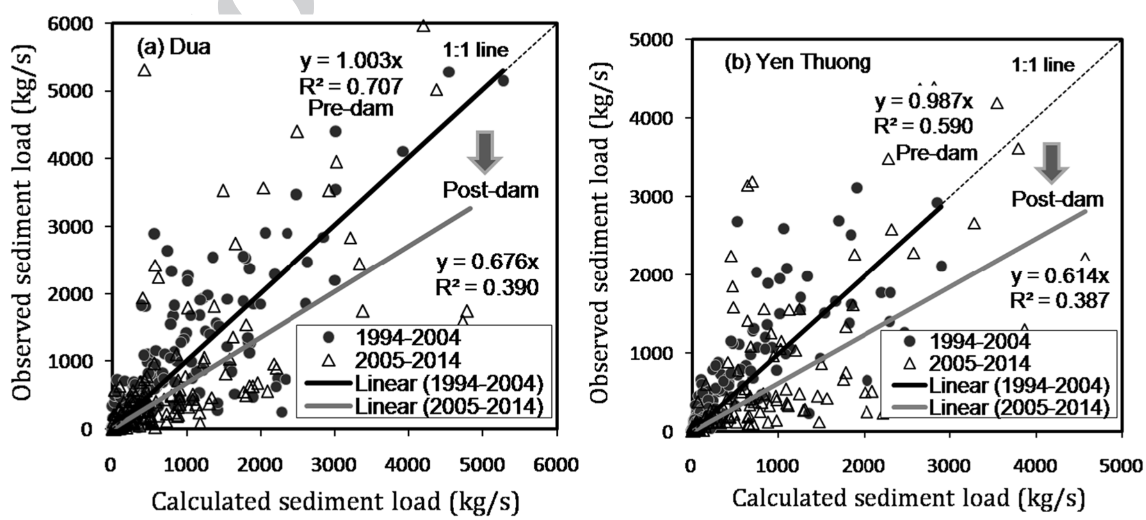

Fig. 3 Comparison of observed and calculated sediment load at Dua (**a**) and Yen Thuong (**b**)

Journal : Large 12665 | Article No : 8394 | Pages : 10 | MS Code : 8394 | Dispatch : 4-7-2019

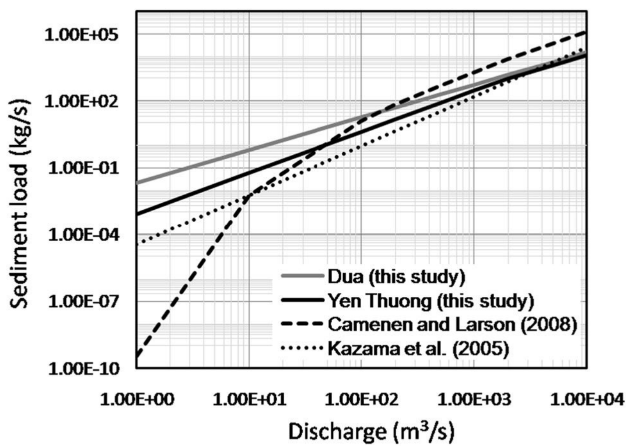

Fig. 4 Loading curves at Dua and Yen Thuong compared with Kazama et al. (2005) and Camenen and Larson (2008)

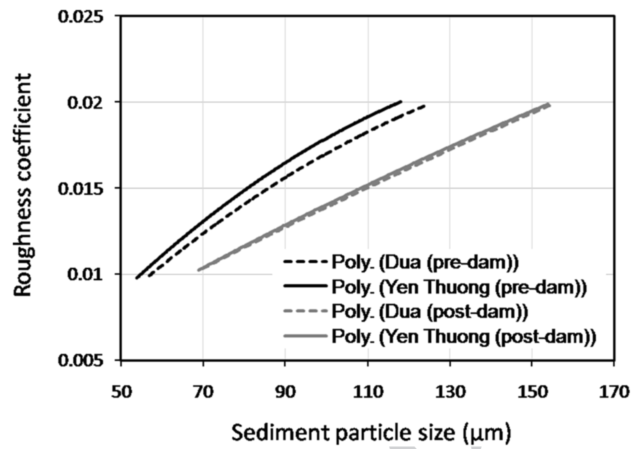

Fig. 5 The relationship between sediment particle size and channel roughness during the pre-dam and post-dam periods

dependence of the sediment load on the cross-sectional area and a slope of the curve exceeding 2. While Eq. (7) holds for slopes between 1.5 and 1.8, the logarithmic profiles and Manning equations are valid partly because of the different particle sizes according to the discharge and partly because of the departure from a steady and uniform flow. Those existing formulas are obtained from laboratory scale tests. However, the present study is fully dependent on the field data and likely reveals a variable particle size in the lower-flow regime with a shallower slope of the loading curve.

Change in the relationship between sediment particle size and channel roughness

In the pre-dam period, the Manning roughness coefficient ranged from 0.01 to 0.02 $m^{-1/3}$ s, and the sediment particle size was selected at the optimal values of the evaluation indices NSE, RSR and PBIAS. The obtained results of sediment size ranged from 57 to 124 µm at the Dua station and 54 to 118 µm at the Yen Thuong station. The calibration process was performed as trials in the post-dam period. The results of the NSE, RSR, and PBIAS indices were approximately 0.39, 0.781, and 14% at the Dua station and 0.39, 0.783, and 13% at the Yen Thuong station. The trade-off in n and D for the pre-dam and post-dam periods is demonstrated in Fig. 5. The results indicate that a new correlation between sediment particle size and channel roughness was established. Dam construction significantly changed the sectional configuration and increased discharge of the river. These changes influenced sediment particle size and channel roughness in the Ca River basin. The climate in the Ca River basin is tropical with monsoonal climate conditions, which results in large variations in annual runoff. Therefore, attaining the equilibrium concentration profile of suspended sediment for a given particle size is not easy. However, after the dams were constructed, the river discharge somehow became regulated and the hydrograph was flattened; the coarsest particles became immobile and the finest particles moved during the dry season. The discharge range (minimum to maximum discharge) narrowed, which is one possible reason why the riverbed got coarser. This situation may have resulted in a significant increase in the roughness (Chien 1985). A similar tendency was reported by Leopold and Maddock (1953) in a laboratory.

Impact of a reservoir on suspended sediment yield

Observed sediment loading curves L_{ss}–Q before and after dam construction in the Ca River basin are presented in Fig. 6. The sediment loading curve decreases from $L_{ss} = 0.0036 \times Q^{1.6659}$ to $L_{ss} = 0.0012 \times Q^{1.76}$ at Dua station and from $L_{ss} = 0.0027 \times Q^{1.704}$ to $L_{ss} = 0.0027 \times Q^{1.591}$ at Yen Thuong station. The annual suspended sediment load was calculated using sediment loading curves for the pre-dam and post-dam periods. The mean annual suspended sediment load decreased by 20% from 4.0×10^6 tons to 3.2×10^6 tons at Dua station and by more than 40% from 6.6×10^6 tons to 3.7×10^6 tons at Yen Thuong station after dam construction. In the pre-dam period, Yen Thuong received about 60% of the suspended sediment from the Upper Dua basin. During the post-dam period, this fraction increased to 86%. The Upper Dua basin covers an area of 20,800 km^2, and the basin between Dua and Yen Thuong (Lower Dua basin) covers an area of 2200 km^2. The mean annual sediment yield of the Upper Dua basin decreased by 20% from 194 to 152 tons/yr/km^2. The annual sediment yield of the Lower Dua basin decreased by more than 80% from 1156 to 231 tons/yr/km^2. These results indicate that the rate of sediment loss

Journal : Large 12665	Article No : 8394	Pages : 10	MS Code : 8394	Dispatch : 4-7-2019

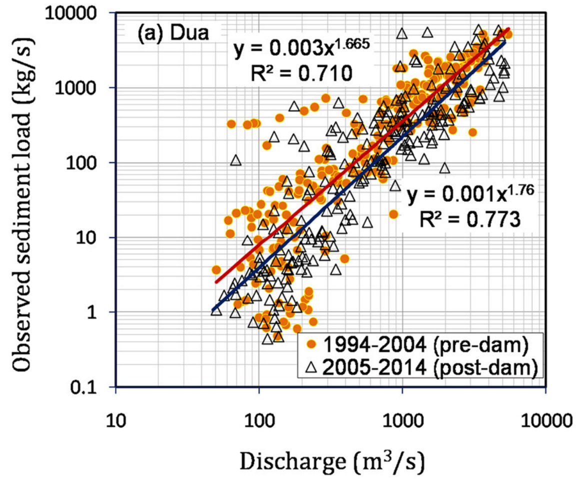

Fig. 6 Observed SS load during the pre-dam and post-dam periods at Dua (**a**) and Yen Thuong (**b**)

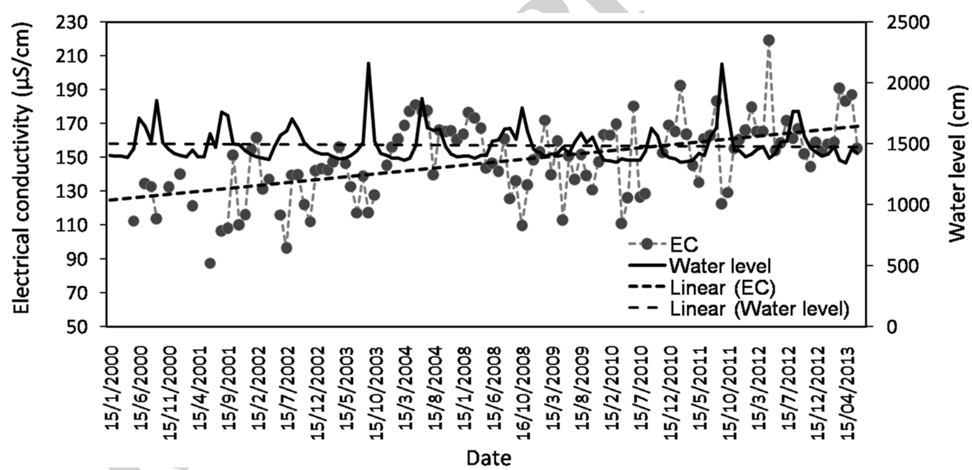

Fig. 7 Long-term electrical conductivity at the Dua station

following impoundments in the lower basin was higher than in the upper basin.

Long-term TDS yields and changes in the TSS–TDS ratio

Long-term EC and water level data at the Dua station are presented in Fig. 7. Electrical conductivity ranged between 88 and 219 μS/cm, and it gradually increased from 2000 to 2013. A negative relationship was observed between EC and water level during runoff peaks. The long-term EC data were converted to TDS concentration for the pre- and post-dam periods. The loading curve of TDS (L_{DS}–Q) in Fig. 8 shows the results of a dissolved solid load in the pre-dam and post-dam periods at the Dua station combined with the TDS load converted from the logger data at both stations. Similar loading curves for TDS were obtained for the pre- and post-dam periods and for the logger data at the Dua station. Therefore, the TDS load, on average, was

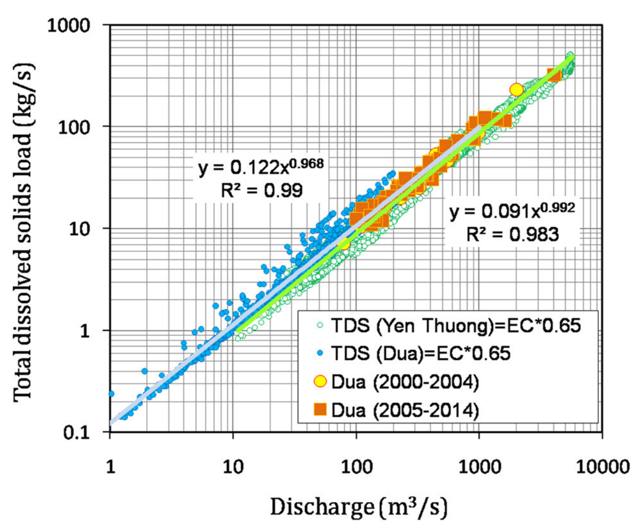

Fig. 8 Loading curve of total dissolved solids at the Dua station

Journal : Large 12665	Article No : 8394	Pages : 10	MS Code : 8394	Dispatch : 4-7-2019

not affected significantly by dam construction. However, this comparison is a very rough estimate.

The dissolved solid loads increased with increasing river flow as a power function $L_{DS} = 0.122 \times Q^{0.968}$ at Dua and $L_{DS} = 0.091 \times Q^{0.992}$ at Yen Thuong. Long-term annual TDS loads were calculated by applying an observed TDS loading curve. The TDS load ranged between 3.6×10^5 and 2.0×10^6 tons/yr at Dua and between 6.1×10^5 and 2.4×10^6 tons/year at Yen Thuong during the time period 1994–2014. The average annual TDS load was 1.3×10^6 tons at Dua and 1.5×10^6 tons at Yen Thuong. On average, Yen Thuong received more than 80% of its TDS load from the Dua basin. The mean annual specific yield of TDS in the Upper Dua basin was 61 tons/yr/km^2; the corresponding value in the Lower Dua basin (between Dua and Yen Thuong) was 124 tons/yr/km^2 for the entire period (1994–2014). The TDS yield in the Lower Dua basin was twofold higher than that of the Upper Dua basin.

The annual TSS–TDS ratio ranged from 1.3 to 4.8, with an average of 2.7 at Dua station, and from 1.3 to 6.9, with an average of 3.2 at Yen Thuong station over the time period 1994–2014. The average TSS–TDS ratio decreased from 3.0 to 2.3 at Dua and from 4.1 to 2.2 at Yen Thuong after dam construction. According to the classification of Milliman and Farnsworth (2011), the Ca River basin is a sediment-dominated river (TSS/TDS > 2). The TSS–TDS ratio at the Yen Thuong station was higher than that at the Dua station during the pre-dam period. However, reservoir construction caused a change in the load of TDS and TSS into rivers, resulting in an altered TSS–TDS ratio. It has been reported that dams decreased sediment loads and caused a shift from a sediment-dominated to dissolved-dominated river in many rivers worldwide (Milliman and Farnsworth 2011).

Conclusions

Suspended sediment transport at two hydrological stations, Dua and Yen Thuong, in the Ca River basin was simulated using semi-empirical forms based on the regime curves for width, depth, and average velocity with roughness coefficient and bulk sediment concentration formulas. Three efficiency criteria—NSE, PBIAS, and RSR—were used to evaluate the suspended sediment predictions during the pre-dam (1994–2004) and post-dam (2005–2014) periods. The comparison of observed and calculated sediment load indicated that the observed sediment decreased after dam construction. Suspended sediment transport was then obtained as a loading curve in terms of the *L*–*Q* equations and compared with theoretical methods presented in the literature. The exponents of the loading curve in this study ranged between 1.46 and 1.85; values exceeding 2.00 have been noted in the literature.

One of the effects of dam construction that we noted was a change in the relationship between Manning's roughness coefficient and sediment particle size. This result was manifested at both stations, and sediment transport was reduced after dam construction, which resulted in reservoir sedimentation. The fraction of lighter solids was suggested to have increased. The mean annual suspended sediment load decreased by 20% from 4.0×10^6 to 3.2×10^6 tons at the Dua station and by more than 40% from 6.6×10^6 to 3.7×10^6 tons at the Yen Thuong station after dam construction. A power-law function with exponents of 0.968 and 0.992 of dissolved solid load was used to calculate the long-term annual TDS at Dua and Yen Thuong, respectively. The TDS load ranged between 0.4 and 2.0 million tons per year at the Dua station and between 0.6 and 2.4 million tons per year at the Yen Thuong station over the time period 1994–2014. The reduction in TSS after dam construction led to a decrease in the TSS–TDS ratio from 3.0 to 2.3 at the Dua station and from 4.1 to 2.2 at the Yen Thuong station.

Acknowledgements This research was financially supported by the Japan Society for the Promotion of Science (Grant no. R11604). The authors would like to express their deep appreciation to Professor Md. Azhar Uddin, Professor Hidetaka Chikamori, and Dr. Mitsuyo Saito of the Graduate School Environmental and Life Science, Okayama University for their helpful comments pertaining to the manuscript and their kind support throughout the research process. The authors also thank Nguyen Xuan Tien of North-Central Hydro-meteorological Centre, Vietnam and the staff at the Dua and Yen Thuong hydrological stations for allowing us to access their gauging records. The authors sincerely thank the anonymous reviewers for their very constructive and useful comments that helped to improve the quality of this manuscript.

References

Amos P, Veale B, Thai NC, Read S (2017) Improving dam and downstream community safety in Vietnam. Hydropower Dams 1. http://www.damwatch.co.nz/newspaper/Vietnam_Damwatch.pdf

Andrews ED (1986) Downstream effects of flaming gorge reservoir on the Green River, Colorado and Utah. Geol Soc Am Bull 97(8):1012–1023. https://doi.org/10.1130/0016-7606(1986)97%3c1012:DEOFGR%3e2.0.CO;2

Brinkmann WLF (1989) Hydrology. In: Lieth H, Werger MJA (eds) Tropical rain forest ecosystems: biogeographical and ecological studies. Elsevier, Amsterdam, pp 89–98

Camenen B, Larson M (2008) A general formula for noncohesive suspended sediment transport. J Coast Res 24(3):615–627. https://doi.org/10.2112/06-0694.1

Celik I, Rodi W (1991) Suspended sediment-transport capacity for open channel flow. J Hydraul Eng 117(2):191–204. https://doi.org/10.1061/(ASCE)0733-9429(1991)117:2(191)

Chien N (1985) Changes in river regime after the construction of upstream reservoirs. Earth Surf Process Landf 10(2):143–159. https://doi.org/10.1002/esp.3290100207

Chikamori H, Heng L, Daniel T (eds) (2012) Catalogue of rivers for Southeast Asia and the Pacific–volume VI. UNESCO-IHP regional steering committee for Southeast Asia and the Pacific. http://unesdoc.unesco.org/images/0021/002170/217039e.pdf

Eiriksdottir ES, Oelkers EH, Hardardottir J, Gislason SR (2017) The impact of damming on riverine fluxes to the ocean: a case study from Eastern Iceland. Water Res 113:124–138. https://doi.org/10.1016/j.watres.2016.12.029

Ferguson RI (1986) Hydraulics and hydraulic geometry. Prog Phys Geogr 10(1):1–31. https://doi.org/10.1177/030913338601000101

Friedl G, Wüest A (2002) Disrupting biogeochemical cycles–consequences of damming. Aquat Sci 64(1):55–65. https://doi.org/10.1007/s00027-002-8054-0

Giang PQ, Giang LT, Toshiki K (2017) Spatial and temporal responses of soil erosion to climate change impacts in a transnational watershed in Southeast Asia. Climate 5(1):22. https://doi.org/10.3390/cli5010022

Habini M (1994) Sediment transport estimation methods in river systems. Dissertation, University of Wollongong. http://ro.uow.edu.au/theses/1263/

Humborg C, Ittekkot V, Cociasu A, Bodungen BV (1997) Effect of Danube River dam on Black Sea biogeochemistry and ecosystem structure. Nature 386:385–388. https://doi.org/10.1038/386385a0

Itakura T, Kishi T (1980) Open channel flow with suspended sediments. J Hydraul Div 106(8):1325–1343

IWRP (2012) Synthesis report of "Review of water resources planning in the Ca River basin" (in Vietnamese). Institute of Water Resources Planning, Directorate of Water Resources, Ha Noi

Kazama S, Suzuki K, Sawamoto M (2005) Estimation of rating-curve parameters for sedimentation using a physical model. Hydrol Process 19(19):3863–3871. https://doi.org/10.1002/hyp.5986

Knighton AD (1977) Short-term changes in hydraulic geometry. In: Gregory KJ (ed) River channel changes. Wiley, Chichester, pp 101–119

Knighton AD (1987) Streamflow characteristics of northeastern Tasmania: II. Hydraulic geometry. Pap Proc Roy Soc Tas 121:125–135

Leopold LB, Maddock T (1953) The hydraulic geometry of stream channels and some physiographic implications. US Government Printing Office, Washington

Lewis LA (1966) The adjustment of some hydraulic variables at discharges less than one cfs. Prof Geogr 18(4):230–234. https://doi.org/10.1111/j.0033-0124.1966.00230.x

Meybeck M (2003) Global analysis of river systems: from Earth system controls to Anthropocene syndromes. Philos Trans R Soc Lond B Biol Sci 358(1440):1935–1955. https://doi.org/10.1098/rstb.2003.1379

Milliman JD, Farnsworth KL (2011) River discharge to the coastal ocean: a global synthesis. Cambridge University Press, New York. https://doi.org/10.1017/CBO9780511781247

Moriasi DN, Arnold JG, Van Liew MW, Binger RL, Harmel RD, Veith TL (2007) Model evaluation guidelines for systematic quantification of accuracy in watershed simulations. Trans ASABE 50(3):885–900. https://doi.org/10.13031/2013.23153

Richards KS (1976) Complex width-discharge relations in natural river sections. Geol Soc Am Bull 87(2):199–206. https://doi.org/10.1130/0016-7606(1976)87%3c199:CWRINR%3e2.0.CO;2

Schall JD, Richardson EV, Morris JL (2008) Introduction to highway hydraulics: hydraulic design series no 4. US Department of Transportation, Federal Highway Administration, Washington. https://www.fhwa.dot.gov/engineering/hydraulics/pubs/08090/HDS4_608.pdf

Thirumalini S, Joseph K (2009) Correlation between electrical conductivity and total dissolved solids in natural waters. Malays J Sci 28(1):55–61. https://doi.org/10.22452/mjs.vol28no1.7

Walton NRG (1989) Electrical conductivity and total dissolved solids—What is their precise relationship? Desalination 72(3):275–292. https://doi.org/10.1016/0011-9164(89)80012-8

Xu J (2007) Trends in suspended sediment grain size in the upper Yangtze River and its tributaries, as influenced by human activities. Hydrol Sci J 52(4):777–792. https://doi.org/10.1623/hysj.52.4.777

Yang Y, Zhang M, Zhu L, Liu W, Han J, Yang Y (2017) Influence of large reservoir operation on water-levels and flows in reaches below dam: case study of the three gorges reservoir. Sci Rep 7(1):15640. https://doi.org/10.1038/s41598-017-15677-y

Publisher's Note Springer Nature remains neutral with regard to jurisdictional claims in published maps and institutional affiliations.

Journal : **Large 12665**	Article No : **8394**	Pages : **10**	MS Code : **8394**	Dispatch : **4-7-2019**